Desalination and Water Treatment
www.deswater.com

doi: 10.1080/19443994.2016.1156027

57 (2016) 25653–25666
November

Taylor & Francis
Taylor & Francis Group

Competitive adsorption of 2,4-dichlorophenoxyacetic acid herbicide and humic acid onto activated carbon for agricultural water management

A.E. Kurtoğlu, G. Atun*

Faculty of Engineering, Department of Chemistry, Istanbul University, 34320 Avcılar-Istanbul, Turkey, email: kurtoglu@istanbul.edu.tr (A.E. Kurtoğlu), Tel. +90 2124737070; Fax: +90 2124737180; email: gultena@istanbul.edu.tr (G. Atun)

Received 8 September 2015; Accepted 15 February 2016

ABSTRACT

Adsorptive removal of herbicide 2,4-dichlorophenoxyacetic acid (2,4-D) and humic acid (HA) from their single- and binary solutions was investigated using powdered activated carbon. Both pore- and film diffusion coefficients for 2,4-D calculated based on two resistance diffusion kinetics were higher than those found for HA both single- and binary component systems. Similar trend was also observed for the rate constants calculated by applying pseudo-second-order kinetic model. The L-shaped isotherm curves converted into H shaped with an increase in the temperature from 288 to 318 K indicating the complete removal of both solutes in dilute solutions. A synergetic effect was observed in low-concentration region in binary systems; however, the combined action of 2,4-D and HA was found to be antagonistic in concentrated solutions. The experimental equilibrium results in single-component systems were better predicted by the Freundlich than the Langmuir isotherm equation. The extended Freundlich isotherm model fit also quite well to the data obtained from binary solutions. The effects of medium acidity and salinity on 2,4-D and HA adsorption process were also examined. Analysis of the pH-dependent adsorption results using Kurbatov approximation suggested that 2,4-D and HA were mainly adsorbed in molecular form on carbon surfaces rather than in their anionic forms.

Keywords: Adsorption; Activated carbon; 2,4-D; Humic acid; Single-component system, binary component system

1. Introduction

The contamination of organic pollutants has become a major concern in the production of safe drinking water. 2,4-dichlorophenoxyacetic acid (2,4-D) is a commonly used herbicide for selective systemic post-emergence control of annual and perennial broad-leaved weeds in cereals, maize, sorghum grassland, orchards, sugarcane, rice, oil palm, cocoa, rubber, and non-crop lands [1,2]. Although its half-life in soil is approximately two weeks, its massive introduction to the environment every year which totals thousands of tones poses a risk for human health and the environment. Adsorption emerges as an attractive option for the removal of organic pollutants among the diversified methods suggested due to its flexibility in design and ease of operation. It has been reported that interactions between phenoxy acid herbicides and other pollutants especially humic matters dissolved

*Corresponding author.

from agricultural soils drastically modify the extraction efficiency [3–8]. Humic acids (HAs) are the mixtures of decomposition products of plants and animals with complex structures and contain large number of functional groups, such as carboxyl (–COOH) and phenolic (–OH) groups [9].

Some of the adsorbents developed for 2,4-D removal are activated carbon (AC) [10–13], polymerin [14], bituminous shale [15], fertilizer and steel industry wastes [16], tire rubber granules [17], zinc–aluminum–chloride-layered double hydroxides [18], organo-clays [19,20], silica gel activated with 3-(trimethoxysilyl)-propylamine [21,22]. Similarly, surfactant-modified bentonite [23], chitosan hydrogel beads [9] have also been used as adsorbent for the removal of HA. However, adsorption on AC is still the most widely used technology regarding the purification of water contaminated by 2,4-D [24–31].

In multi-component systems, previously adsorbed species can either act as additional binding sites or occupy the same binding sites as the subsequent species to be adsorbed, resulting in enhanced or retarded adsorption of the subsequent species [9]. It will be interesting to compare adsorption behavior of 2,4-D and HA onto AC in single- and binary component systems.

2. Materials and methods

2.1. Adsorbate specifications

The herbicide 2,4-dichlorophenoxyaceticacid (2,4-D) was supplied from Atabay Pharmaceutical Products Inc. (Turkey) and used without purification. Its melting point, solubility in water at 298 K, and pK_a value are 413.5 K, 620 mg L^{-1} [32], and 2.6 [33], respectively. HA was provided from Aldrich. HAs which behave as mixtures of dibasic acids, have a $pK_{a,1}$ value around 4 for ionization of carboxyl groups and a $pK_{a,2}$ around 8 for ionization of phenolate groups [34].

Three-dimensional (3-D) molecular structures of 2,4-D and a typical HA, having a various components such as quinone, phenol, catechol, and sugar moieties were created using the semi-empirical PM 3 method in the Hyper Chem 8.0 package program presented in Fig. 1.

2.2. Adsorbent specifications

Powdered activated carbon (PAC) used in this study was supplied from Anhui Technology I/E Co. Ltd. The analysis of the compound yielded the following data: moisture: 3.26 (wt.%), ash: 5.46 (wt.%),

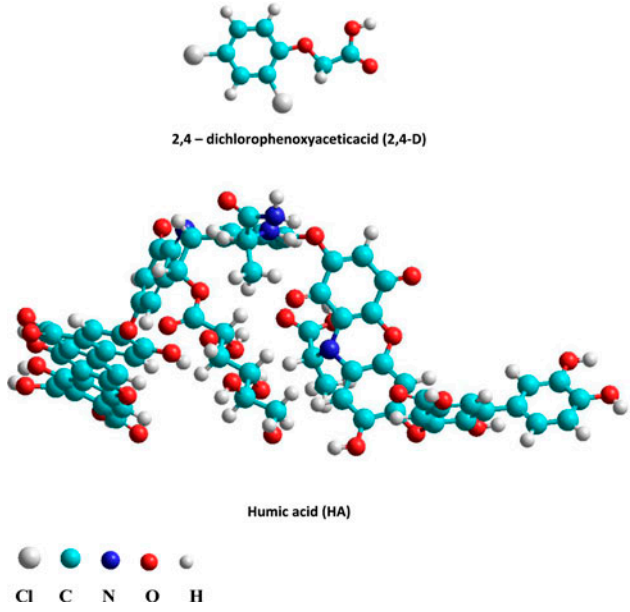

Fig. 1. Three-dimensional (3-D) molecular structures of the studied compounds.

surface area: 319 m^2 g^{-1}, particle size range: 0.015–0.075 mm, average particle size: 0.071 mm, and density: 0.44 g cm^{-3}. The reported values of point of zero charge (pH_{pzc}) and surface site concentration of adsorbent were 8.81 and 0.51 mol kg^{-1}, respectively [35].

2.3. Infrared spectral measurements

The surface functional groups of the PAC were characterized by diffuse reflectance Fourier-transform infrared (FT-IR) spectroscopy using a Bruker Alpha-T model spectrometer. The FT-IR spectra of the saturated PAC with 2,4-D, HA and their mixtures were compared with the bare surface and the free molecules in Fig. 2.

2.4. Concentration determination

Concentrations of the solutions were measured using UV-1800 Shimadzu UV–vis spectrophotometer. UV spectra were recorded in the wavelength range of 200–400 nm employing quartz cells with a pathway of 1 cm. The concentrations of 2,4-D and HA in the solutions were determined from the peaks located at around a λ_{max} of 283 and 254 nm, respectively. The representative UV spectra in 220–320 nm range were shown in Fig. 3 for the solutions of 10 mg L^{-1}. Correlation coefficients (r^2) of absorbance vs. C curves used for concentration determination were higher than 0.999 both single- and binary component systems.

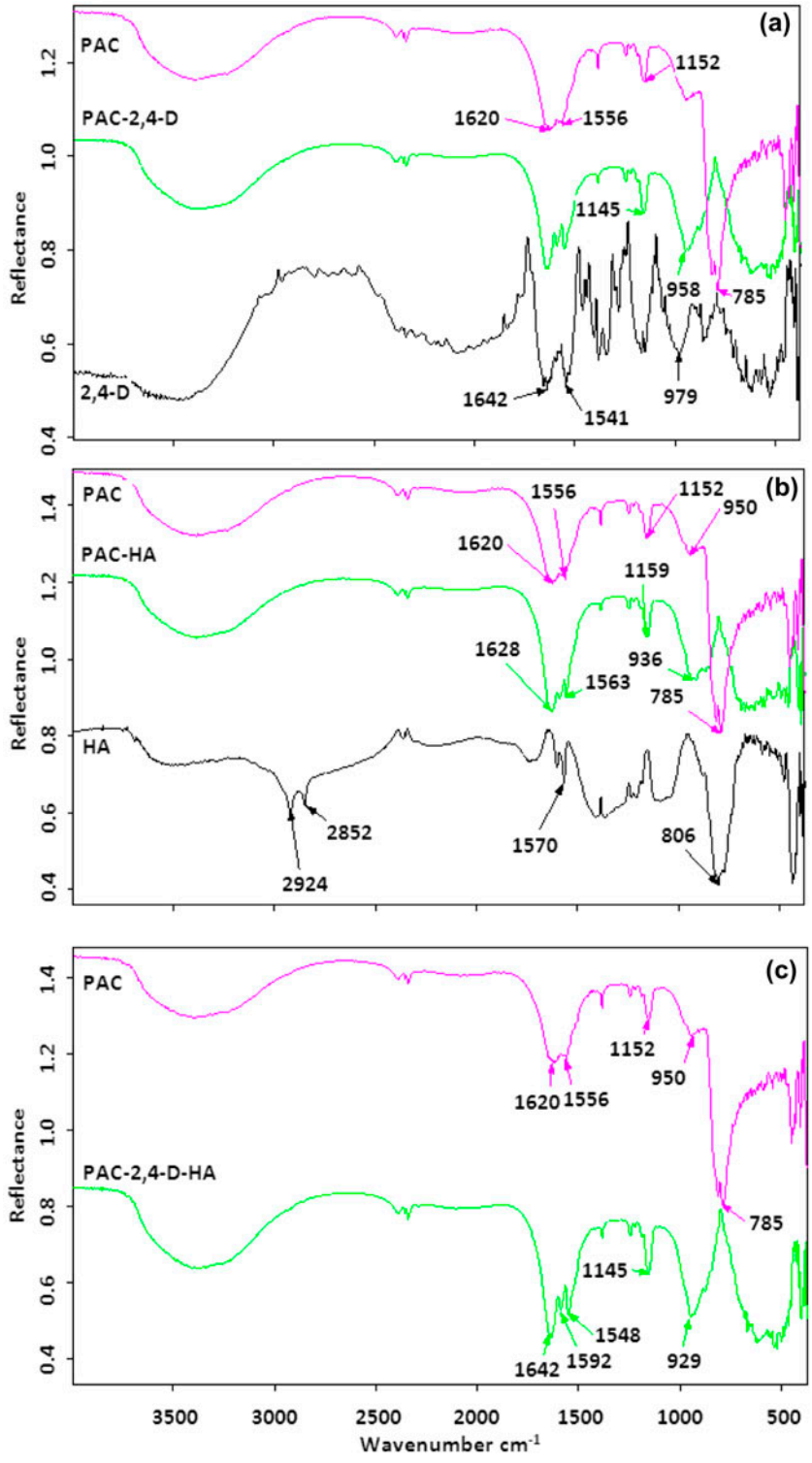

Fig. 2. A comparison of FT-IR spectra of (a) PAC, PAC-2,4-D, free 2,4-D, (b) PAC, PAC-HA, free HA, and (c) PAC, PAC-2,4-D-HA.

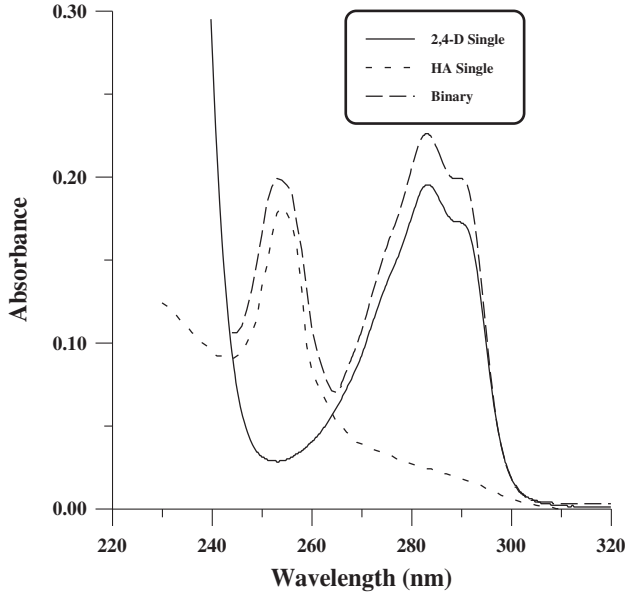

Fig. 3. UV spectra of 2,4-D and HA in single and binary solutions (C = 10 mg L^{-1}).

2.5. Kinetic studies

The equilibrium time of adsorption process was determined by the time-dependent studies. Time dependency of 2,4-D and HA adsorption in single-component systems was studied at 25 ($C_{0,1}$) and 50 mg L^{-1} ($C_{0,2}$) initial concentrations, respectively.

Kinetic experiments were carried out in a water-jacketed Pyrex cell using 50 mL of the solutions at a given concentration. Solutions were continuously stirred with a magnetic stirrer at 298 K after adding 0.25 g of the PAC. The solutions were separated by centrifugation at 7,000 rpm at time intervals.

Kinetic studies in binary solutions were performed at 0.25 mg L^{-1} initial concentrations for both components.

The amount of adsorbed solute (q_t) at any time was calculated from the concentration changes during adsorption process using the following equation:

$$q_t = (C_0 - C_t)\frac{V}{m} \quad (1)$$

where C_0 and C_t are the solute concentrations at initial and time t (in mg L^{-1}), V is the solution volume, and m is the adsorbent mass.

The change of q_t with time was depicted in Fig. 4(a) and (b) for 2,4-D and HA adsorption in single- and binary component systems, respectively.

As shown in Fig. 4(a), adsorption equilibrium was established in a few minutes for 2,4-D in single system, whereas HA adsorption slowed down after 2 hours and attained to the an equilibrium in 4 h. The optimal process time was selected as 4 h for equilibrium experiments. Although the equilibration time was much lower for binary system, all experiments were conducted under similar conditions.

2.6. Equilibrium studies

The single- and binary component solutions in the concentration range of 5–100 mg L^{-1} were shaken with the PAC in a thermostatic shaker for 4 h until the equilibrium was reached. Adsorbent dosage was selected as 1 g L^{-1} (i.e. 0.01 g/0.01 L) to obtain relevant data for construction of the adsorption isotherms. The ratio of initial concentrations of 2,4-D and HA in binary systems was 1.

In order to evaluate thermodynamic parameters, the experiments were performed at 288, 298, 308, and 318 K as well.

The effect of the medium acidity on 2,4-D and HA adsorption process was studied in 50 mg L^{-1} single and binary solutions of 2,4-D and HA prepared in 10^{-3}, 10^{-2}, and 10^{-1} M HCl solutions at 1 g L^{-1} adsorbent dosage. Initial and final pHs of the solutions (pH_i and pH_e) were measured using a Jenway pH meter connected to a combined glass electrode.

The effect of salinity on the adsorption process was also investigated in 10 mL 10^{-1} M NaCl solutions containing 10^{-3}, 10^{-2}, and 10^{-1} M HCl under similar conditions with the pH experiments.

3. Results and discussion

3.1. FT-IR analysis

The adsorption ability of the PAC depends on the porosity and the chemical reactivity of functional groups at the surface. Fig. 2(a)–(c) shows the FT-IR spectra of the PAC before and after loading of 2,4-D, HA and their mixtures, respectively. The changes in the spectra would give information about interactions between the molecules and the surface functional groups.

The broadband in the range of 3,200–3,650 cm^{-1} on the PAC spectrum is due to the absorption of water molecules as a result of an O–H stretching mode of hydroxyl groups and adsorbed water as well as the hydrogen-bonded –OH group of alcohols and phenols. The band at 1,635 cm^{-1} specifies C=O results from the stretching vibrations of amide groups, aldehydes, and ketones. The N–O stretching vibrations in nitroalkanes occur near 1,556 cm^{-1} (asymmetrical) and 1,390 cm^{-1} (symmetrical). The peaks at 1,246 and 1,152 cm^{-1} can

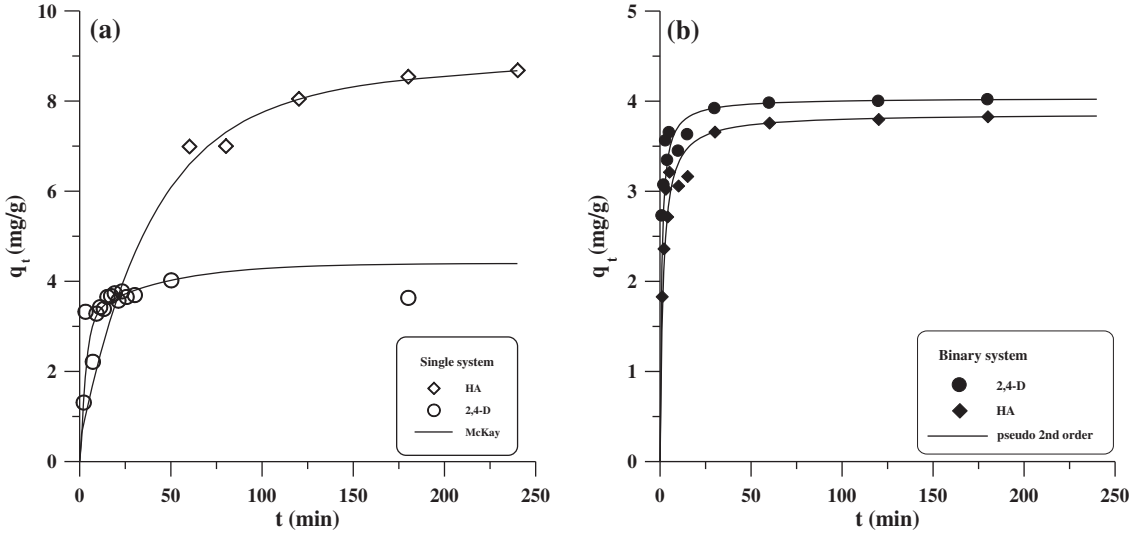

Fig. 4. Determination of the process time at 5 g L^{-1} adsorbent dosage: (a) for single systems of 2,4-D and HA at 25 and 50 mg L^{-1} initial concentrations, respectively, and (b) for binary component system at 25 mg L^{-1} initial concentration of both solutes (T = 298 K).

be attributed to C–O of phenolic groups and OH of COOH, respectively. The shoulder at 950 cm^{-1} is due to terminal alkyne groups. The strongest peak at 785 cm^{-1} is assigned to benzene rings with two or three adjacent H and its shoulder at 821 cm^{-1} is due to aromatic C–H stretching.

The bands at 1,642 and 1,541 cm^{-1}, as shown by the curve of free 2,4-D in Fig. 2(a), stem from C=O stretching vibrations and the asymmetrical stretching of $–COO^{–}$ groups, respectively. The C–O and C–Cl stretches appear in the 1,300–1,000 cm^{-1} and 850–450 cm^{-1} region, respectively [36].

The peaks at 2,924 and 2,852 cm^{-1} in the free HA spectrum in Fig. 2(b) are the result of the aliphatic groups substituted to the benzene ring. The C=C and C=N stretching vibrations of the aromatic rings and the N=N bonds appear in the 1,600–1,400 cm^{-1} region. The peaks located at the lower wave numbers belong to C–N and C–H vibrations in the rings. The peak at 806 cm^{-1} is attributed to aromatic C–H stretching [37].

The sharpest peak at 785 cm^{-1} assigned to aromatic C–H stretching completely disappeared on the spectra of all loaded sorbents. This may be attributed to molecular adsorption by the Van der Waals forces [38]. The slight shift from 1,152 to 1,146 cm^{-1} may be the indication of H bond formation between phenolic and carboxylic groups of the PAC and 2,4-D. The shift of the peak at 950 cm^{-1} to lower frequencies suggests that HA interacts with terminal alkyne groups. As can be seen from Fig. 2(c), similar interactions are also observed on the PAC spectrum loaded both molecules.

3.2. Adsorption kinetics

As shown in Fig. 4(a) and (b), an initial fast stage is followed by a slower process for 2,4-D and HA adsorption systems. The mass transfer stage involves three major steps as follows: (i) external film diffusion across the boundary layer, (ii) adsorption at a surface site, and (iii) internal mass transfer within the particle based on a pore or intraparticle diffusion [39]. The rate of adsorption process may be determined by one or more of these steps. The kinetic results were analyzed by applying McKay [40] model based on two-resistance diffusion process [41] and pseudo-second-order kinetic model assuming chemisorption of adsorbate on adsorbent [42].

3.2.1. McKay model

McKay equation, which assumes film- and intraparticle diffusion, can be written in the following form [40]:

$$\ln(1 - F_t) = -k(C_t + \overline{C}_t)t \quad (2)$$

where F_t is the adsorbed fraction and $\overline{C}_t$ is the solute concentration in the solid phase at time t (in mg L^{-1}).

The representative $\ln(1 - F_t) = f(t)$ curves plotted according to McKay equation for single-component systems are shown in Fig. 5. The curves are analyzed as follows. The linear portion is extrapolated to t = 0. There is a straight line obtained subtracting the

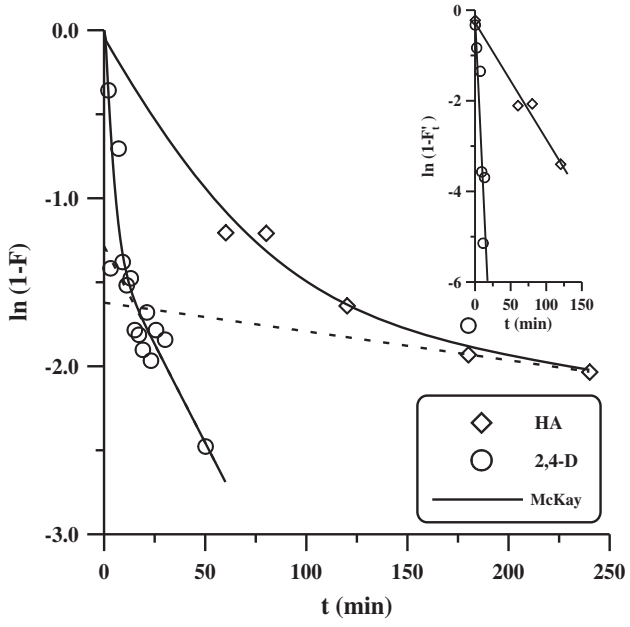

Fig. 5. Application of the McKay model to the kinetic data for single-component systems: (a) McKay plot for calculation of k_2 and D_p. The inset: McKay plot for calculation of k_1 and D_f (adsorbent dosage: 5 g L^{-1}, $C_{0,1}$ = 25 and $C_{0,2}$ = 50 mg L^{-1}, T = 298 K).

extrapolated line from the original curve shown in the inset in Fig. 5, whose slope is correlated to the rate constant of initial fast process (k_1, in L mg^{-1} s^{-1}).

The film diffusion coefficient D_f (in m^2 s^{-1}) can be calculated from the following relation using the k_1 values [43,44]:

$$D_f = k_1 \frac{V\delta\overline{C}_\infty}{S} \tag{3}$$

where V is the solution volume, δ is the thickness of liquid film which is assumed to be equal to mean particle radius, S is the specific surface area of the adsorbent and $\overline{C}_\infty$ is the adsorbate concentration in solid phase at infinite time of adsorption process.

The rate constant k_2 (in L mg^{-1} s^{-1}) corresponding to the slow process is determined from the slope of extrapolated straight lines in Fig. 5 according to the following equation [43,44]:

$$\ln(1 - F_t) = A - k_2(C_t + \overline{C_t})t \tag{4}$$

When the particle diffusion contributes to the adsorption process, the following equation can be used to obtain adsorbed fraction assuming a radial diffusion [43,44]:

$$F_t = 1 - \sum_{n=1}^{\infty} \frac{6\alpha(\alpha+1)}{9 + 9\alpha + \alpha^2 q_n^2} e^{-D_p q_n^2 t/r_0^2} \tag{5}$$

Thus,

$$\ln(1 - F_t) = A - \frac{D_p q_1^2}{r_0^2} t \tag{6}$$

where $A = \ln[6\alpha(\alpha+1)]/(9 + 9\alpha + \alpha^2 q_1^2)$, r_0 is the mean radius of the adsorbent particles, q_n's are the nonzero roots of $\tan q_n = (3q_n)/(3 + \alpha q_n^2)$ and $\alpha = (3V)/(4\pi r_0^3 n)$ is the volume ratio of external solution to the adsorbent, and n is the number of solid particles. The constant k_2 can be correlated to D_p with a combination of Eqs. (4) and (6) as follows [43,44]:

$$D_p = k_2 \frac{(C_t + \overline{C}_t) r_0^2}{q_1^2} \tag{7}$$

The kinetic parameters, k_1,k_2, D_f, and D_p for 2,4-D and HA in single- and binary component systems were presented in Table 1. The D_f values reported for HA adsorption on hexadecyl-trimethylammonium (HDTMA) chloride-modified bentonite were in the range of (3.24–4.97) × 10^{-11} m^2 s^{-1} for the adsorbent particles of 0.096 mm size, whereas D_p values were observed to be (2.03–3.46) × 10^{-14} m^2 s^{-1} at 303 K [23]. Cho et al. [27] have reported diffusion coefficients of 2,4-D in single-component systems on three types of granulated ACs. The reported values of the external film mass transfer coefficients, k_f, were in the range of 2.5 × 10^{-5} and 5.00 × 10^{-5} m s^{-1}, while the pore diffusion coefficients, D_p, and surface diffusion coefficients, D_s, were observed to change between (0.62–1.50) × 10^{-9} m^2 s^{-1} and (1.58–1.90) × 10^{-13} m^2 s^{-1}, respectively.

The reported values of diffusion coefficients in the literature for 2,4-D and HA adsorption in single-component system are comparable with the data presented in Table 1. These results suggest that the rate of adsorption processes may be controlled by both film and intraparticle diffusion. Using the D_f and D_p values in Table 1, calculated F_t vs. t curves according to McKay model can be compared with the experimental points in Fig. 5 for single-component systems. Experimental data are well predicted by McKay model for both single- and binary component systems.

3.2.2. Pseudo-second-order kinetic model

The pseudo-second-order kinetic model proposed by Ho and McKay can be written as follows [42]:

Table 1
Kinetic parameters for 2,4-D and HA adsorption in single- and binary component systems

		McKay model						Pseudo-second-order model		
	System	$k_1 \times 10^5$ (L mg^{-1} s^{-1})	$D_f \times 10^{10}$ (m^2 s^{-1})	r^2	$k_2 \times 10^7$ (L mg^{-1} s^{-1})	$D_p \times 10^{14}$ (m^2 s^{-1})	r^2	k_s (g mg^{-1} min^{-1})	q_e (mg g^{-1})	r^2
2,4-D	Single	22.27	4.46	0.79	155.95	2.25	0.83	0.063	4.83	0.99
HA		0.86	0.38	0.96	5.72	0.12	1.00	0.004	9.66	1.00
2,4-D	Binary	7.14	1.50	0.71	2.12	0.05	1.00	0.283	4.03	1.00
HA		3.61	1.35	0.96	1.61	0.04	1.00	0.156	3.86	1.00

$$\frac{dq_t}{dt} = k_s(q_e - q_t)^2 \quad (8)$$

where k_s is the rate constant (g mg min^{-1}) and q_e is the amount of solute adsorbed at equilibrium conditions (mg g^{-1}). The integration of Eq. (8) results in the following equation for the boundary conditions, $q_t = 0$ at $t = 0$ and $q_t = t$ at $t = t$:

$$q_t = \frac{k_s q_e^2 t}{1 + k_s q_e t} \quad (9)$$

The kinetic data for both single- and binary component systems fit well to linear form of Eq. (10) presented below:

$$\frac{t}{q_t} = \frac{1}{k_s q_e^2} + \frac{1}{q_e} t \quad (10)$$

The t/q_t vs. t plot is depicted in Fig. 6 for binary component system, and the parameters q_e and k_s obtained from the slope and the intercepts of the straight lines are listed in Table 1 for both systems. A comparison of experimental points and the calculated curves using pseudo-second-order kinetic model parameters is shown in Fig. 4(b). As can be seen from the figure, the modeled curves are consistent with experimental points.

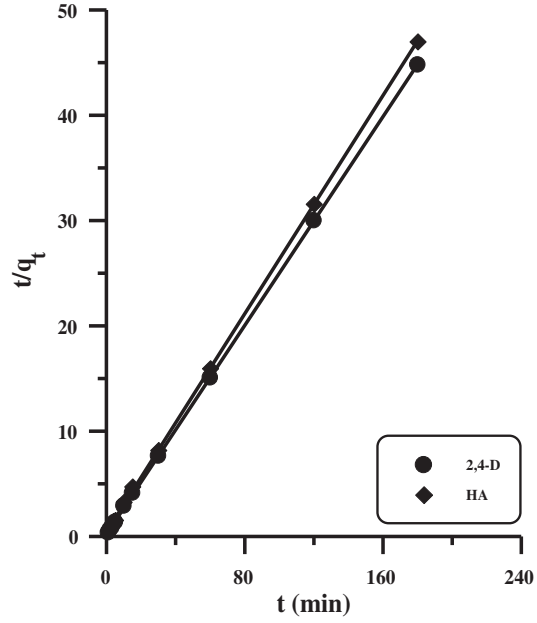

Fig. 6. The pseudo-second-order kinetic model plots for binary component system (adsorbent dosage: 5 g L^{-1}, $C_{0,1}$ = 25 and $C_{0,2}$ = 25 mg L^{-1}, T = 298 K).

3.3. Adsorption equilibria

3.3.1. Effect of temperature on adsorption equilibria in single-component systems

The adsorption isotherms of 2,4-D and HA in single-component systems are shown in Fig. 7(a) and (b). According to Giles classification, L-shaped isotherm curves are observed for adsorption of both solutes at 288 and 298 K [45]. This type of isotherms indicates that both 2,4-D and HA have reasonable high affinity for PAC. The curves shift toward the left side as the temperature increases and they convert into the H-shaped isotherms. This type of curves is an extreme case of the L-shaped isotherm reflecting very high affinity of adsorbate for the adsorbent. Equilibrium concentrations close to zero at low initial concentration region indicating that both solutes are completely removed by the PAC.

The experimental data in Fig. 7(a) and (b) have been analyzed according to the well-known Freundlich and the Langmuir isotherm equations.

The Freundlich expression based on a heterogeneous surface and unlimited number of unreacted adsorption sites is commonly given as:

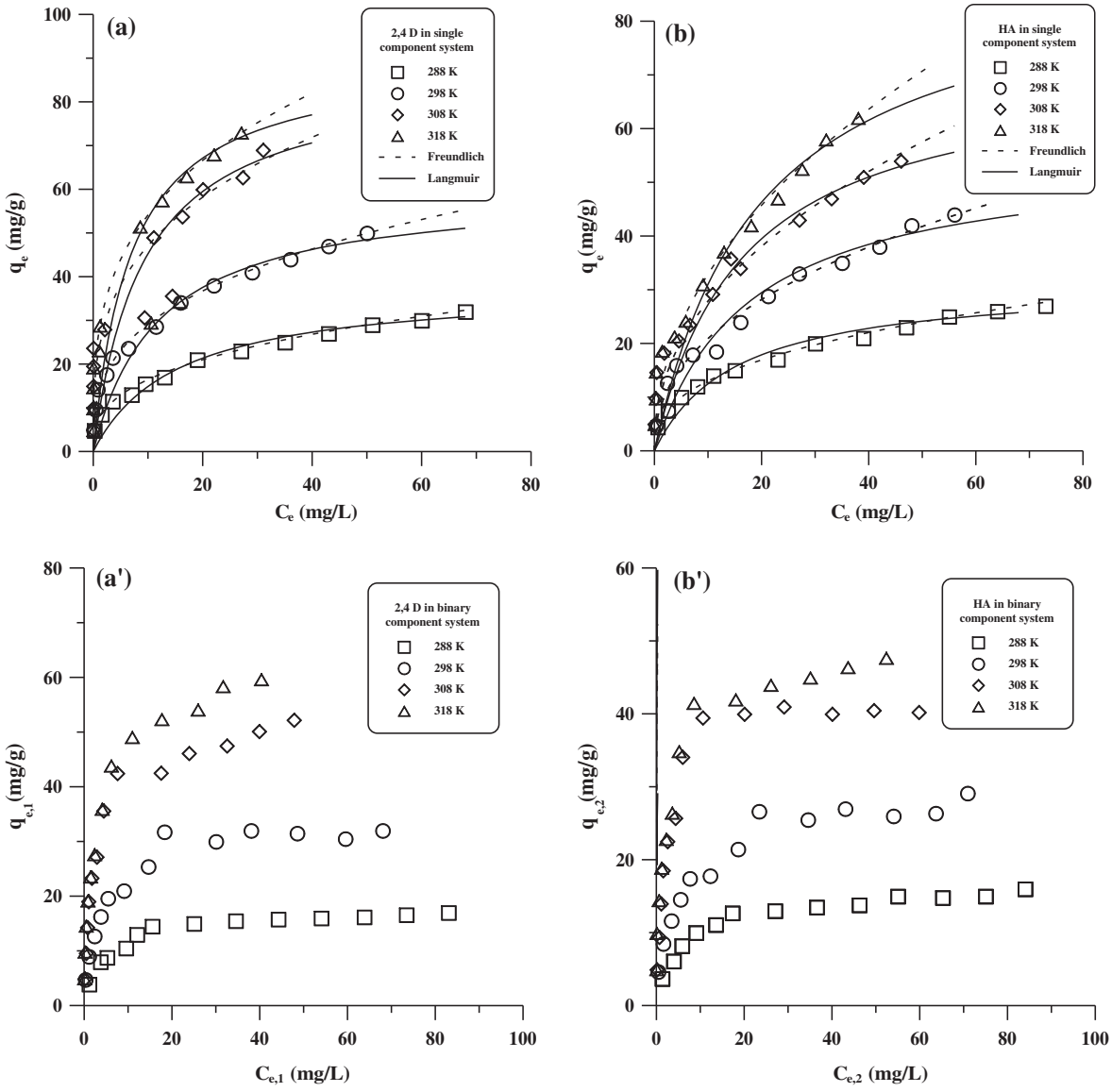

Fig. 7. Adsorption isotherms at different temperatures (a) 2,4-D and (b) HA in single-component systems (dashed and solid curves were drawn according to Freundlich and Langmuir models, respectively). (a´) 2,4-D and (b´) HA in binary component systems (adsorbent dosage: 1 g L^{-1}, C_0 = 5–100 mg L^{-1}).

$$q_e = K_F C_e^{n_F} \tag{11}$$

where K_F is the Freundlich constant, which is a comparative measure of the adsorption capacity of the adsorbent, and n_F is an empirical constant related to surface heterogeneity.

Another useful model is the Langmuir isotherm equation, which assumes the monolayer coverage on an energetically identical homogeneous adsorbent surface. The Langmuir equation can be written as follows:

$$q_e = \frac{K_L q_m}{1 + K_L C_e} C_e \tag{12}$$

where K_L is the adsorption equilibrium constant related to the binding energy and q_m is the monolayer capacity.

The isotherm constants calculated by nonlinear regression method are listed in Table 2. A comparison of standard deviations shows that the Freundlich isotherm fits better to experimental data over the whole adsorption range. These results are consistent with the

Table 2
Freundlich and Langmuir isotherm parameters for 2,4-D and HA adsorption in single component systems

	Freundlich				Langmuir		
	T (K)	K_F (mg g^{-1})/(mg L^{-1})^n	n	σ	q_m (mg g^{-1})	K_L (L mg^{-1})	σ
2,4-D	288	7.3	0.352	0.043	37.8	0.065	0.350
	298	13.5	0.325	0.037	60.1	0.083	0.471
	308	23.3	0.305	0.434	86.9	0.109	0.714
	318	27.1	0.300	0.442	90.4	0.144	0.735
HA	288	5.4	0.380	0.024	31.5	0.066	0.267
	298	7.8	0.431	0.075	55.3	0.057	0.314
	308	9.9	0.452	0.097	71.9	0.061	0.532
	318	11.0	0.475	0.098	91.7	0.051	0.542

reported studies on 2,4-D and HA adsorption onto carbon samples with different origin [26,27,31].

The values of $0 < n_F < 1$ for both systems are an indication of favorable adsorption and a heterogeneous surface. The Langmuir monolayer capacities for 2,4-D and HA increase in the range of 37.8–90.4 mg g^{-1} and 31.5–91.7 mg g^{-1} as the temperature increases from 288 to 318 K.

3.3.2. Thermodynamic parameters

Thermodynamic functions can be calculated from the following equations using dimensionless adsorption equilibrium constant K° evaluated from Langmuir parameter K_L:

$$\Delta G^\circ = -RT \ln K^\circ \tag{13}$$

$$\ln K^\circ = \frac{\Delta S^\circ}{R} - \frac{\Delta H^\circ}{RT} \tag{14}$$

The values of standard enthalpy (ΔH°) and entropy changes (ΔS°) estimated from the linear relation between $\ln K^\circ$ and $1/T$ as 20.29 kJ mol^{-1} and 0.16 kJ mol^{-1} K^{-1} for the adsorption of 2,4-D, and −5.22 kJ mol^{-1} and 0.07 kJ mol^{-1} K^{-1} for the adsorption of HA, respectively. Standard free energy changes (ΔG°) for 2,4-D and HA adsorption were calculated as −28.12 kJ mol^{-1} and −27.27 kJ mol^{-1}. The exothermic nature of the process suggested that the interactions between HA molecules and PAC surface were stronger compared to endothermic 2,4-D adsorption process. The negative values of ΔG° indicate that both processes were thermodynamically feasible and spontaneous. The values of ΔG° are in the mid of physical and chemical adsorption [46]. Although the adsorption process of 2,4-D was endothermic in nature, its free energy change was more negative due to higher entropy change. This means that the driving force of the spontaneity was controlled by the entropy change. The positive values of ΔS° indicated that both 2,4-D and HA molecules were randomly distributed on the PAC surface.

3.3.3. Effect of temperature on adsorption equilibria in binary component systems

Adsorption isotherms of 2,4-D and HA in binary component systems are presented in Fig. 7(a′) and (b′). Although amount of each solute adsorbed from binary solutions is slightly lower than that of single-component system at 288 and 298 K, synergetic effects are observed at higher temperatures in low-concentration region. However, adsorption process becomes antagonistic at higher concentrations.

Since single-component isotherms are better described by the Freundlich equation, its extended form can be applied to analyze the equilibrium results in binary solutions. The extended Freundlich isotherm can be written as follows [47]:

$$q_{e,1} = \frac{K_{F,1} C_{e,1}^{n_1+x_1}}{C_{e,1}^{x_1} + y_1 C_{e,2}^{z_1}} \tag{15}$$

$$q_{e,2} = \frac{K_{F,2} C_{e,2}^{n_2+x_2}}{C_{e,2}^{x_2} + y_2 C_{e,1}^{z_2}} \tag{16}$$

where $K_{F,1}$, n_1, $K_{F,2}$, and n_2 are the Freundlich isotherm constants of the first and the second components in single-solute systems and other six parameters (x_1, y_1, z_1 and x_2, y_2, z_2) are extended Freundlich constants for binary solute systems. $q_{e,1}$ and $q_{e,2}$ are the equilibrium adsorption of the first

and the second components, and $C_{e,1}$ and $C_{e,2}$ are their equilibrium concentrations.

The equilibrium adsorption of 2,4-D and HA was calculated by nonlinear regression from Eqs. (15) and (16) by minimizing standard deviations between observed and calculated $q_{e,i}$ values:

$$\sigma = \left[\frac{1}{n_e - 2}\sum_{i=1}^{n}\left(\frac{q_{e,i,exp} - q_{e,i,cal}}{q_{e,i,exp}}\right)^2\right]^{1/2} \quad (17)$$

where n_e is the number of experimental observations, subscripts "exp" and "cal" indicate the experimental and calculated values of the solute adsorbed.

The calculated amounts of 2,4-D adsorbed ($q_{e,1,cal}$) and HA ($q_{e,2,cal}$) together with isotherm parameters (x_1, y_1, z_1 and x_2, y_2, z_2) are presented in Table 3. As can be seen from the σ values, the extended Freundlich isotherm fits quite well to the equilibrium data of both solutes in binary solutions.

3.4. Effect of pH on adsorption

The effect of pH on the removal efficiency of 2,4-D in single- and binary component systems was compared with that of HA in the absence and presence of NaCl in Table 4.

As can be seen from Table 4, adsorption efficiency increases with decreasing pH. These results suggest that both 2,4-D and HA can be adsorbed in anionic form on positively charged surface sites at the pHs below pH_{pzc} of 8.81 as well as in molecular form with hydrophobic interactions on carbon surface. When the initial pH is close to the pK_a (i.e. 2.6) or higher, the equilibrium pH of the solution increases, and in some cases, it goes to neutral values where 2,4-D presents in anionic form. When the initial pH is below pK_a, the equilibrium pH does not show significant variations and slightly decreases. It clearly suggests two distinctive sorption processes. The data presented in Table 4 can be utilized in a model developed by Kurbatov to predict anion adsorption at varying solution pHs [48].

Table 3
Calculated amounts of 2,4-D and HA adsorbed in binary component systems according to extended Freundlich model and the parameters used in calculations (adsorbent dosage: 1 g L^{-1})

	$q_{e,1,cal}$ (mg g^{-1})				$q_{e,2,cal}$ (mg g^{-1})			
C_0 (mg L^{-1})	288 K	298 K	308 K	318 K	288 K	298 K	308 K	318 K
5	3.8	4.9	4.8	4.9	3.8	4.4	4.8	5.0
10	5.8	8.0	8.9	9.4	5.6	7.7	8.9	9.9
15	6.6	10.4	11.1	15.8	6.4	10.4	10.7	11.0
20	8.1	12.3	12.6	17.4	7.4	12.4	12.1	11.9
25	8.8	13.9	15.7	18.9	8.6	13.9	14.6	15.7
30	9.6	16.5	19.3	22.5	9.4	16.5	18.5	19.7
40	11.4	19.4	22.8	27.5	10.9	19.0	21.1	23.2
50	12.8	20.9	28.0	31.4	12.1	20.5	26.5	28.9
60	13.9	24.8	38.2	37.7	13.1	23.2	32.9	39.3
70	15.0	26.8	42.8	44.6	13.9	24.9	37.0	43.8
80	15.9	29.1	47.9	51.0	14.7	26.8	40.3	46.4
90	16.7	31.2	51.5	54.4	15.4	28.1	42.2	48.6
100	17.4	32.6	55.0	59.2	16.0	29.0	43.7	49.0
	x_1				x_2			
	0.008	0.065	0.205	0.320	0.010	−0.090	−0.350	−0.355
	y_1				y_2			
	0.980	0.700	0.800	0.550	0.550	0.200	0.010	0.006
	z_1				z_2			
	0.010	0.040	0.010	0.210	0.100	0.200	0.600	0.850
	σ				σ			
	0.215	0.205	0.239	0.169	0.161	0.126	0.248	0.228

Table 4
pH dependence of 2,4-D and HA adsorption in single- and binary component systems on PAC in the presence and absence of NaCl and the parameters derived from Kurbatov approximation (adsorbent dosage: 1 g L^{-1}, C_0 = 50 mg L^{-1}, equilibration time: 4 h, T = 298 K)

		HCl/M	NaCl/M	pH_i	pH_e	Removal %	x	pK	r
Single-component system	2,4-D	10^{-3}	–	2.55	6.75	62.90	0.35	−6.30	1.00
		10^{-2}	–	2.29	2.91	89.54			
		10^{-1}	–	1.25	0.93	95.77			
		10^{-3}	10^{-1}	2.54	5.85	63.44	0.41	−6.53	0.97
		10^{-2}	10^{-1}	1.97	3.38	92.08			
		10^{-1}	10^{-1}	0.87	0.90	95.69			
	HA	10^{-3}	–	6.24	7.98	67.50	0.13	−5.12	0.99
		10^{-2}	–	2.25	5.75	72.70			
		10^{-1}	–	0.92	1.04	87.00			
		10^{-3}	10^{-1}	6.33	7.47	85.99	0.10	−5.89	0.70
		10^{-2}	10^{-1}	2.25	4.98	94.48			
		10^{-1}	10^{-1}	0.84	0.94	93.65			
Binary component system	2,4-D	10^{-3}	–	3.79	7.01	76.65	0.17	−5.50	0.64
		10^{-2}	–	2.90	3.80	79.30			
		10^{-1}	–	1.91	1.67	91.58			
		10^{-3}	10^{-1}	4.43	6.64	64.81	0.13	−5.04	0.75
		10^{-2}	10^{-1}	2.82	3.70	85.47			
		10^{-1}	10^{-1}	1.64	1.48	81.19			
	HA	10^{-3}	–	3.79	7.01	73.80	0.16	−5.28	0.61
		10^{-2}	–	2.9	3.8	72.42			
		10^{-1}	–	1.91	1.67	90.12			
		10^{-3}	10^{-1}	4.43	6.64	62.72	0.15	−5.11	0.77
		10^{-2}	10^{-1}	2.82	3.7	85.89			
		10^{-1}	10^{-1}	1.64	1.48	81.60			

The macroscopic semi-empirical model of the effects of pH on anion adsorption on the solid surface is based on the following expression:

$$RH + xH^+ + A_n^- \overset{K}{\leftrightarrow} RH_{x+1}^+ - A_n^- \tag{18}$$

where RH represents surface functional group not associated with the anion, A_n^-, x corresponds the number of protons uptake per mole of anion removed from solution and $RH_{x+1}^+ - A_n^-$ is the anion surface site complex. The equilibrium constant K for the reaction is given by:

$$K = \frac{[RH_{x+1}^+ - A_n^-]}{[RH][H^+]^x[A_n^-]} \tag{19}$$

This equation can be arranged as follows:

$$\log K = \log \frac{[RH_{x+1}^+ - A_n^-]}{[RH][A_n^-]} - x \log[H^+] \tag{20}$$

$$Q = \frac{[RH_{x+1}^+ - A_n^-]}{[RH][A_n^-]} \tag{21}$$

$$\log K = \log Q - x \log[H^+] \tag{22}$$

$$pQ = pK + xpH \tag{23}$$

The parameters K and x can be used to characterize the anion adsorption properties of a given adsorbate–adsorbent system which can be computed from the slope and intercept of pQ vs. pH plot (known as Kurbatov plot) in Fig. 8. The values of Q were evaluated from experimental bulk solution concentrations at equilibrium. The values of K and x calculated from Fig. 8 were also tabulated in Table 4. A noninteger x value suggests that 2,4-D is also adsorbed in molecular form on the surface of the AC.

The removal efficiencies of 2,4-D and HA were slightly higher in the presence of 10^{-1} M NaCl suggesting that uptake of Na^+ ions contributes on positive surface charge of the adsorbent and anionic species are favored by the adsorbent.

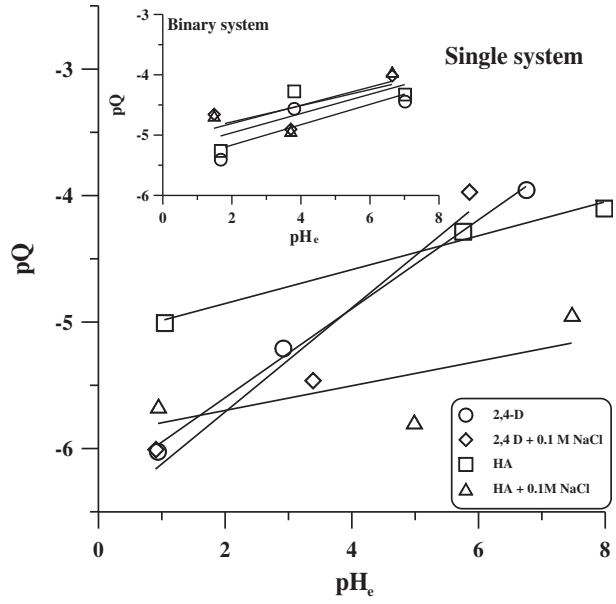

Fig. 8. Kurbatov plots for 2,4-D and HA in single- and binary component systems (in the inset) (adsorbent dosage: 1 g L^{-1}, C_0 = 50 mg L^{-1}, equilibration time: 4 h, T = 298 K).

4. Conclusions

Equilibrium and kinetic parameters for adsorptive removal of 2,4-D and HA on PAC were evaluated from the data obtained in single- and binary component systems in the concentration range of 5–100 mg L^{-1}.

The solutes were completely removed from their single-component systems at low concentrations and elevated temperatures.

Equilibrium adsorption increased with increasing temperature for both solutes in single and binary solutions, and the results were described well by the Freundlich isotherm equation and its extended form, respectively. The L-shaped isotherm curves shifted toward the left side as the temperature increased from 288 to 318 K and converted into the H shaped indicating that the solutes have higher affinity for the PAC at higher temperatures in low-concentration region.

Although amounts of adsorbed solutes were close to each other under equilibrium conditions, adsorption rate of 2,4-D was higher than that of HA in single- and binary component systems.

Adsorption rate was controlled by film and intraparticle diffusion or chemisorption in the present systems. It can be concluded that rate-limiting steps were intraparticle diffusion and chemisorption for 2,4-D and HA, respectively.

Removal efficiency increased with decreasing pH. Amounts of 2,4-D and HA adsorbed were higher in the presence of NaCl in the same acidity medium.

The results obtained from single- and binary adsorption systems fit well to the theoretical kinetic and equilibrium models. The model parameters calculated in this study may be useful for the design of an herbicide removal plant in the presence of HA.

References

[1] J. Villaverde, M. Kah, C.D. Brown, Adsorption and degradation of four acidic herbicides in soils from southern Spain, Pest, Manage. Sci. 64 (2008) 703–710.
[2] J.B. Alam, K. Dikshit, M. Bandyophadyay, Effect of different inorganic and organic compounds on sorption of 2,4-D and atrazine, J. Environ. Sci. Health B 37 (2002) 54–560.
[3] A. Farenhorst, I.M. Saiyed, T.B. Goh, P. McQueen, The important characteristics of soil organic matter affecting 2,4-dichlorophenoxyacetic acid sorption along a catenary sequence, J. Environ. Sci. Health, Part B 45 (2010) 204–213.
[4] M.P. GarcÍa De Llasera, A. RodrÍguez-Castillo, L.E. Vera-Avila, Relative influence of the dissolved humic material on the solid-phase extraction efficiency of pesticides from environmental water, J. Environ. Sci. Health, Part B 42 (2007) 615–627.
[5] J.S. Ra, S.Y. Oh, B.C. Lee, S.D. Kim, The effect of suspended particles coated by humic acid on the toxicity of pharmaceuticals, estrogens, and phenolic compounds, Environ. Int. 34 (2008) 184–192.
[6] L.J. Merini, V. Cuadrado, A.M. Giulietti, Spiking solvent, humidity and their impact on 2,4-D and 2,4-DCP extractability from high humic matter content soils, Chemosphere 71 (2008) 2168–2172.
[7] L.J. Merini, V. Cuadrado, C.G. Flocco, A.M. Giulietti, Dissipation of 2,4-D in soils of the Humid Pampa region, Argentina: A microcosm study, Chemosphere 68 (2007) 259–265.
[8] S. Moret, J.M. Sanchez, V. Salvado, M. Hidalgo, The evaluation of different sorbents for the preconcentration of phenoxyacetic acid herbicides and their metabolites from soils, J. Chromatogr. A 2005 (1099) 55–63.
[9] W.L. Yan, R. Bai, Adsorption of lead and humic acid on chitosan hydrogel beads, Water Res. 39 (2005) 688–698.
[10] M. Zahoor, M. Mahramanlioglu, Removal of 2,4-D from water, using various adsorbents in combination with ultrafiltration, Fresenius Environ. Bull. 20 (2011) 2508–2513.
[11] M. Pirsaheb, A. Dargahi, S. Hazrati, M. Fazlzadeh-davil, Removal of diazinon and 2,4-dichlorophenoxy-acetic acid (2,4-D) from aqueous solutions by granular-activated carbon, Desalin. Water Treat. 52 (2014) 4350–4355.

[12] V.O. Njoku, M. Asif, B.H. Hameed, 2,4-Dichlorophenoxyacetic acid adsorption onto coconut shell-activated carbon: isotherm and kinetic modeling, Desalin. Water Treat. 55 (2015) 132–141.
[13] K. Kuśmierek, M. Sankowska, A. Świątkowski, Kinetic and equilibrium studies of simultaneous adsorption of monochlorophenols and chlorophenoxy herbicides on activated carbon, Desalin. Water Treat. 52 (2014) 178–183.
[14] F. Sannino, M. Iorio, A. De Martino, M. Pucci, C.D. Brown, R. Capasso, Remediation of waters contaminated with ionic herbicides by sorption on polymerin, Water Res. 42 (2008) 643–652.
[15] N. Ayar, B. Bilgin, G. Atun, Kinetics and equilibrium studies of the herbicide 2,4-dichlorophenoxyacetic acid adsorption on bituminous shale, Chem. Eng. J. 138 (2008) 239–248.
[16] V.K. Gupta, I. Ali, Suhas, V.K. Saini, Adsorption of 2,4-D and carbofuran pesticides using fertilizer and steel industry wastes, J. Colloid Interface Sci. 299 (2008) 556–563.
[17] J.B. Alam, A.K. Dikshit, M. Bandyopadhayay, Evaluation of thermodynamic properties of sorption of 2,4-D and atrazine by tire rubber granules, Sep. Purif. Technol. 42 (2005) 85–90.
[18] A. Legrouri, M. Lakraimi, A. Barroug, A. De Roy, J.P. Besse, Removal of the herbicide 2,4-dichlorophenoxyacetate from water to zinc–aluminium–chloride layered double hydroxides, Water Res. 39 (2005) 3441–3448.
[19] G. Akçay, M. Akçay, K. Yurdakoç, Removal of 2,4-dichlorophenoxyacetic acid from aqueous solutions by partially characterized organophilic sepiolite: Thermodynamic and kinetic calculations, J. Colloid Interface Sci. 281 (2005) 27–32.
[20] G. Akçay, K. Yurdakoç, Removal of various phenoxyalkanoic acid herbicides from water by organoclays, Acta Hydrochim. Hydrobiol. 28 (2000) 300–304.
[21] A.G.S. Prado, C. Airoldi, Adsorption, preconcentration the herbicide 2,4-dichlorophenoxyacetic acid, Fresenius J. Anal. Chem. 371 (2001) 1028–1030.
[22] A.G.S. Prado, C. Airoldi, Adsorption, preconcentration and separation of cations on silica gel chemically modified with the herbicide 2,4-dichlorophenoxyacetic acid, Anal. Chim. Acta 432 (2001) 201–211.
[23] T.S. Anırudhan, M. Ramachandran, Surfactant-modified bentonite as adsorbent for the removal of humic acid from wastewaters, Appl. Clay Sci. 35 (2007) 276–281.
[24] B.H. Hameed, J.M. Salman, A.L. Ahmad, Adsorption isotherm and kinetic modeling of 2,4-D pesticide on activated carbon derived from date stones, J. Hazard. Mater. 163 (2009) 121–126.
[25] P. Chingombe, B. Saha, R.J. Wakeman, Effect of surface modification of an engineered activated carbon on the sorption of 2,4-dichlorophenoxy acetic acid and benazolin from water, J. Colloid Interface Sci. 297 (2006) 434–442.
[26] Z. Aksu, E. Kabasakal, Batch adsorption of 2,4-dichlorophenoxy-acetic acid (2,4-D) from aqueous solution by granular activated carbon, Sep. Purif. Technol. 35 (2004) 223–240.
[27] S.Y. Cho, S.J. Kim, T.Y. Kim, H. Moon, S.J. Kim, Adsorption characteristics of 2,4-dichlorophenoxyacetic acid and 2,4-dinitrophenol in a fixed bed adsorber, Korean J. Chem. Eng. 20 (2003) 365–374.
[28] C. Namasivayam, D. Kavitha, Adsorptive removal of 2,4-dichlorophenol from aqueous solution by low-cost carbon from an agricultural solid waste: Coconut coir pith, Sep. Sci. Technol. 39 (2004) 1407–1425.
[29] J.W. Ma, H. Wang, F.Y. Wang, Z.H. Huang, Adsorption of 2,4-dichlorophenol from aqueous solution by a new low-cost adsorbent-activated bamboo charcoal, Environ. Sci. Technol. 33 (1999) 1200–1206.
[30] D. Kalderis, D. Koutoulakis, P. Paraskeva, E. Diamadopoulos, E. Otal, J. Valle, C. Fernández-Pereira, Adsorption of polluting substances on activated carbons prepared from rice husk and sugarcane bagasse, Chem. Eng. J. 144 (2008) 42–50.
[31] E. Lorenc-Grabowska, G. Gryglewicz, Adsorption of lignite-derived humic acids on coal-based mesoporous activated carbons, J. Colloid Interface Sci. 284 (2005) 416–423.
[32] M. Al Kuisi, Adsorption of dimethoate and 2,4-D on Jordan Valley soils and their environmental impacts, J. Environ. Jeol. 42 (2002) 666–671.
[33] R. Celis, M.C. HermosÍn, L. Cox, J. Cornejo, Sorption of 2,4-dichlorophenoxyacetic acid by model particles simulating naturally occurring soil colloids, Environ. Sci. Technol. 33 (1999) 1200–1206.
[34] F.J. Stevenson, Humus Chemistry: Genesis. Composition Reactions. Wiley, New York, NY, 1994.
[35] N. Ayar, G. Atun, Modeling of adsorption kinetics and equilibria of acid dyes onto activated carbon in single- and binary-component systems, Toxicol. Environ. Chem. 96 (2015) 1012–1028.
[36] J. Li, M. Jiang, H. Wu, Y. Li, Addition of modified bentonites in polymer gel formulation of 2,4-D for ıts controlled release in water and soil, J. Agric. Food Chem. 57 (2009) 2868–2874.
[37] M. Tatzber, M. Stemmer, H. Spiegel, C. Katzlberger, G. Haberhauer, A. Mentler, M.H. Gerzabek, FTIR-spectroscopic characterization of humic acids and humin fractions obtained by advanced NaOH, $Na_4P_2O_7$, and Na_2CO_3 extraction procedures, J. Plant Nutr. Soil Sci. 170 (2007) 522–529.
[38] K. Mahapatra, D.S. Ramteke, L.J. Paliwal, Production of activated carbon from sludge of food processing industry under controlled pyrolysis and its application for methylene blue removal, J. Anal. Appl. Pyrol. 95 (2012) 79–86.
[39] Y.S. Ho, G. McKay, Sorption of dye from aqueous solution by peat, Chem. Eng. J. 70 (1998) 115–124.
[40] H. Mckay, Kinetics of exchange reactions, Nature 142 (1938) 997–998.
[41] G. McKay, Application of surface diffusion model to the adsorption of dyes on bagasse pith, Adsorption 4 (1998) 361–372.
[42] Y.S. Ho, G. McKay, Pseudo-second order model for sorption processes, Process Biochem. 34 (1999) 451–465.
[43] T.C. Huang, F.N. Tsai, Kinetic studies on the isotopic exchange of calcium ion and calcium carbonate, J. Inorg. Nucl. Chem. 32 (1970) 17–31.

[44] T.C. Huang, K.Y. Li, S.C. Hoo, Mechanism of isotopic exchange reaction between calcium ion and calcium oxalate, J. Inorg. Nucl. Chem. 34 (1972) 47–55.
[45] C.H. Giles, D. Smith, A.A. Huitson, A general treatment and classification of the solute adsorption isotherm. I. Theoretical, J. Colloid Interface Sci. 47 (1974) 755–765.
[46] G. Crini, P.M. Badot, Application of chitosan, a natural aminopolysaccharide, for dye removal from aqueous solutions by adsorption processes using batch studies: A review of recent literature, Prog. Polym. Sci. 33 (2008) 399–447.
[47] W. Fritz, E.U. Schluender, Simultaneous adsorption equilibria of organic solutes in dilute aqueous solutions on activated carbon, Chem. Eng. Sci. 29 (1974) 1279–1282.
[48] A.R. Wilson, L.W. Lion, Y.M. Nelson, M.L. Shuler, W.C. Ghiorse, The effects of pH and surface composition on Pb adsorption to natural freshwater biofilms, Environ. Sci. Technol. 35 (2001) 3182–3189.